A Self-powered Wireless Sensor Node for Structural Health Monitoring

Dao Zhou[a], Na Kong[a], Dong Sam Ha[a], and Daniel J. Inman[b]
[a]Department of Electrical and Computer Engineering, Virginia Polytechnic Institute and State University, Blacksburg, VA, USA 24061;
[b]Department of Mechanical Engineering, Virginia Polytechnic Institute and State University, Blacksburg, VA, USA 24061

ABSTRACT

We developed a self-powered wireless autonomous Structural Health Monitoring (SHM) sensor node using a Texas Instruments MSP430 evaluation board. The sensor node employs a PZT (Lead Zirconate Titanate) based impedance method, which saves power by eliminating a digital-to-analog-converter (DAC) for generation of an excitation signal and an analog-to-digital converter (ADC) for sensing the response. The sensor node wakes up at a predetermined interval, performs an SHM operation, and reports the result to the host computer wirelessly. The sensor node consumes only 0.3 J and is powered up by the energy harvested from vibrations, often available from infrastructures. The power management circuit integrated with a piezoelectric cantilever with the size of 50 mm x 31.8 mm generate up to 2.9 mW under 0.5g (rms) base acceleration, which is sufficient to run an SHM operation on every two minutes.

Keywords: energy harvesting, self-powered, SHM, piezoelectric generator, impedance method, wireless sensor

1. INTRODUCTION

Structural health monitoring (SHM) is the process of monitoring and assessing the health condition of aerospace, civil, and mechanical infrastructures such as aircrafts, railroads, bridges, buildings and windmills using a sensing system integrated into the structure. SHM is capable of detecting, locating, and quantifying various types of damage such as cracks, holes, corrosion, delaminations, and loose joints. In the SHM process, the structure is monitored through an array of sensors, and then damage-sensitive features are extracted from the measurement data for assessing the damages.

A wireless SHM sensor node is highly desirable, but replacement or recharge of batteries is a major bottleneck for wide deployment of wireless sensor nodes (WSNs). Moreover, while the size of electronic circuitry shrinks thanks to the advent of VLSI technology, batteries are often the most bulky devices for wireless sensor nodes. The energy harvested from a variety of ambient sources (heat, solar, wind, vibration, radio frequency radiation) provides possible means to recharge the battery or eliminate them entirely.

We developed a self-powered wireless sensor node for SHM. The two design objectives are reduction of power consumption for SHM and increase of the efficiency for energy harvesting. Our sensor node employs an impedance based SHM method, which drastically reduces power dissipation by eliminating the digital-to-analog-converter (DAC) for generation of an excitation signal and the analog-to-digital converter (ADC) for sensing the response. The low average power consumption for our sensor node offers a possibility to power up the sensor node with energy harvested from the ambient. Vibrations are an energy source available for some infrastructures. A power management circuit is developed to harvest vibration energy using a piezoelectric cantilever. The circuit generates a regulated DC output from a piezoelectric generator, while matching the source impedance dynamically. The energy harvesting system is integrated into the SHM sensor to make it self-powered.

2. PROPOSED SYSTEM DESIGN

Our self-powered SHM system contains two major subsystems, an SHM sensor detecting damage of a structure and an energy harvesting system harvesting energy from ambience. The block diagram of the system is shown in Figure 1. The front end part is an energy harvesting system. A piezoelectric cantilever generates AC power, and a power conditioning circuit regulates the output voltage to charge a battery. A storage element such as a battery is necessary, as most ambient

Health Monitoring of Structural and Biological Systems 2010, edited by Tribikram Kundu,
Proc. of SPIE Vol. 7650, 765010 · © 2010 SPIE · CCC code: 0277-786X/10/$18 · doi: 10.1117/12.847334

energy sources are fluctuating. A microcontroller controls the power conditioning circuit dynamically to maximize the power efficiency. The back end part is an SHM sensor node. The microcontroller generates the excitation signal , which actuates a PZT (Lead Zirconate Titanate) patch attached on the structure under test. Note that the microcontroller is shared by both systems to save power. The objectives of the design are to maximize the harvested source energy and minimize the power consumption of the SHM node. The following sections describes how we attempted to achieve the two objectives.

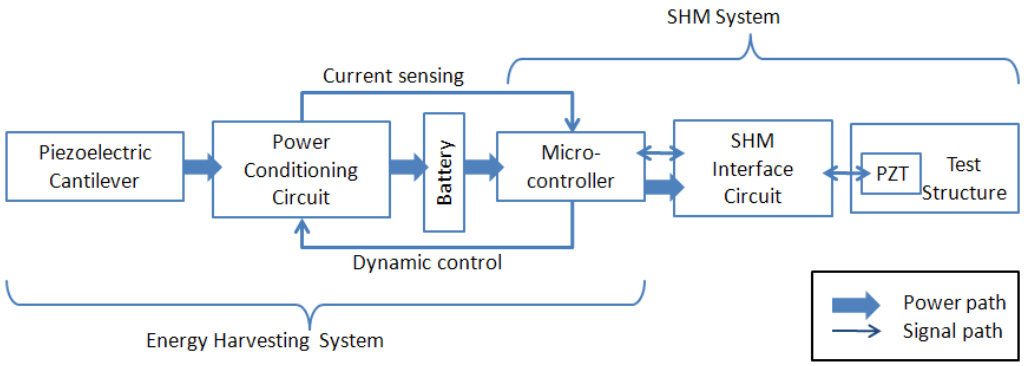

Figure 1: System architecture

3. LOW-POWER SHM SENSOR NODE

The impedance method based on piezoelectric wafers such as PZT is effective for in situ local damage detection. Unlike passive sensing methods, the impedance-based method combines sensing with actuation, which sweeps a certain frequency range to measure the impedance profile of a structure. In this section, we present three methods employed for low-power design of our wireless SHM sensor node. The first method is on-board data processing to reduce the radio transmission time, which substantially reduces the power dissipated by the radio. The second method is elimination of a digital-to-analog converter (DAC) for excitation signal generation, and the third one is elimination of an analog-to-digital converter (ADC) for response sensing.

3.1 On-board data processing

The major source of power consumption for a wireless sensor node is the radio. For example, a microcontroller unit TI MSP430 from Texas Instruments dissipates 3 mW under a low-power operation mode, while a low-end radio CC2500 from Texas Instruments embedded in the sensor node dissipates 65 mW during transmission. So, it is essential to reduce the radio transmission time for a low-power wireless SHM sensor node. We adopt an on-board data processing approach for our SHM sensor node, which processes the data on the board and sends only the final outcome (healthy or damaged) of the SHM operation to the control center. So, the radio for our sensor node transmits only three bytes of data, including the outcome of the SHM operation and the ambient temperature. Other measures adopted for our sensor node is to cut off the power for the analog interface circuit (which drives a PZT patch) in the sleep mode in addition to put the microcontroller in low power mode.

3.2 Elimination of a DAC for generation of an excitation signal

A sinusoidal signal sweeping a certain frequency range is usually used to excite a PZT patch for the impedance method. Generation of a sinusoidal signal usually relies on a DAC. Sampled values of a sinusoidal signal are pre-stored in a memory, and a processor reads the pre-stored data and applies it to a DAC to generate the corresponding analog signal. This method is straightforward, but it requires a DAC and a large memory space for a large-frequency sweeping range.

Our method is to employ a rectangular pulse train rather than a sinusoidal signal. A rectangular pulse train illustrated in Figure 1 (a) has the duty cycle of 0.5, and its fundamental frequency (which is given as $1/t_p$, where t_p is the pulse period) sweeps a certain desired frequency range. The Fourier transform of a pulse train with a pulse period t_p and a duty cycle of 0.5 has odd harmonics kf_o, $k=1, 3, 5$ ..., where $f_o = 1/t_p$. Figure 1 (b) illustrates frequency components of a pulse train with the fundamental frequency ranging from 40 kHz to 50 kHz. The magnitude of the third harmonic is about 33 percent of the fundamental frequency, and the fifth one about 20 percent.

A rectangular pulse train is digital, and hence a processor can directly generate such a signal. Since generation of a rectangular pulse train does not require a DAC, it reduces power consumption of an SHM sensor node. One potential issue is existence of harmonics on the signal. Note that our interest is to detect the difference between the baseline impedance profile and a currently measured one. Since both profiles are under the subject of the same frequency terms, the sensitivity for detecting the difference may not be affected by harmonics. Further, harmonic terms decrease rapidly, and some harmonic terms may be out of the interested frequency range. Our experimental results reveal that use of a rectangular pulse train does not incur any noticeable deterioration of the performance for the impedance method [1][2].

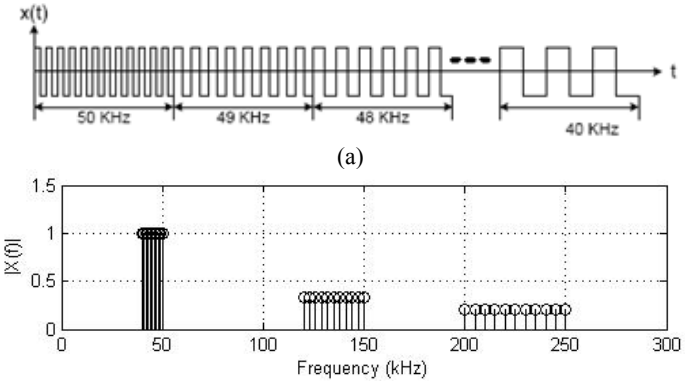

Figure 2. Rectangular pulse train (a) time domain (b) frequency domain

3.3 Elimination of an ADC for response signal sensing

Existing methods such as Analog Device's impedance analyzer chips sample the response signal using an ADC and performs a Fast Fourier Transform (FFT) to extract the impedance component of the frequency. A typical ADC used for an SHM system consumes large power, possibly next to a radio and a processor, and FFT is also computationally intensive to increase power dissipation. Our method is to eliminate an ADC and the FFT operation by sensing the phase, not the magnitude, of the response signal.

The electrical admittance is expressed as $Y(jf) = G(f) + jB(f)$, where $G(f)$ and $B(f)$ are conductance and susceptance terms, respectively. It is known that the conductance term of a PZT patch is more sensitive to damage [3]. Let $G_{base}(f)$ denote the baseline conductance obtained from a healthy structure and $G_{SUT}(f)$ be the conductance of a structure under test (SUT). The difference of the two conductance terms $G_{base}(f) - G_{SUT}(f)$ is used for existing impedance-based SHM systems to detect damage. Our earlier work showed that

$$G_{base}(f) - G_{SUT}(f) \approx C \sin[\phi_{base}(f) - \phi_{SUT}(f)] \tag{1}$$

where C is a constant, and $\phi_{base}(f)$ and $\phi_{SUT}(f)$ are the phase of the baseline admittance and the SUT admittance, respectively. Expression (1) suggests that difference of the phases, instead of the conductance $G(f)$'s, can be sensed for the impedance method.

The phase of admittance $\phi(f)$ for a frequency f can be expressed as in (2), where $T_d(f)$ is the time difference between the voltage and the current:

$$\phi(f) = 2\pi f \times T_d(f) \tag{2}$$

When both the voltage and current are represented as binary signals, the phase difference of the two signals is obtained using an exclusive-OR (XOR) operation as illustrated in Figure 3. A processor can measure the time delay by sampling the output of the XOR operation at a system clock frequency, where the system clock frequency is typically much higher than the frequency f of the admittance under consideration.

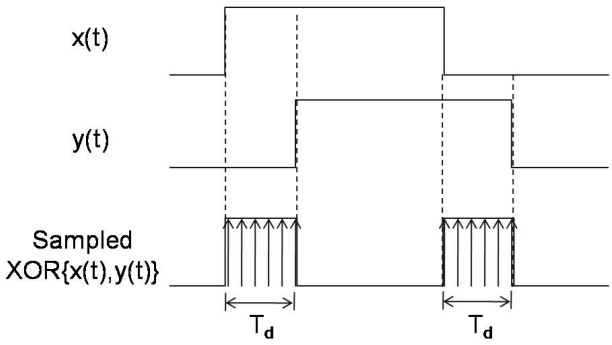

Figure 3. Phase difference measured by sampling the output of the XOR operation.

Figure 4 shows a simplified circuit diagram for a phase measurement. A rectangular pulse train $V_{in}(t)$ is buffered by an opamp and applied to the PZT attached to the structure. The output of opamp OP3 is the current through the PZT, which is delayed in time by a certain amount. The reference voltage V_{ref} shifts the DC level of the applied input voltage, and it is set to one half of the peak-to-peak voltage of input signal $V_{in}(t)$. OP4 is a comparator, which shapes the current waveform into digital. The XOR gate detects the difference between the input voltage and the current through the PZT. OP1 is necessary to drives a highly capacitive PZT, and OP2 is added to delay the excitation signal by the same amount as OP1.

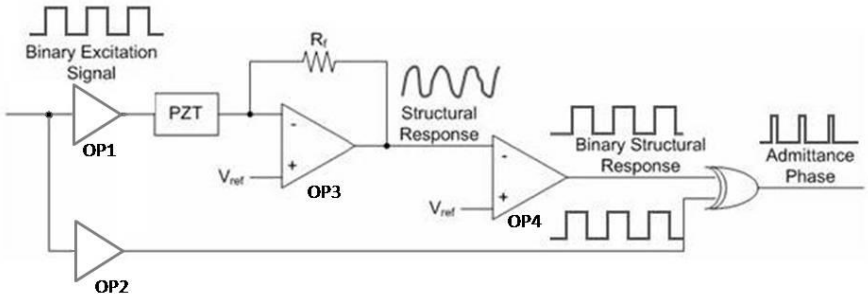

Figure 4. Phase measurement circuit.

4. MAXIMUM POWER TRACKING ENERGY HARVESTING SYSTEM

Due to the intermittence of energy sources and a low operation duty cycle of wireless sensors, a storage element is usually necessary to store surplus energy while the sensor node sleeps and function as an energy buffer when the sensor node is active. A power conditioning circuit is necessary to regulate the raw power harvested from ambient sources before its application to sensor nodes. The efficiency of power conditioning circuits is a key design requirement and affected by several factors including power losses associated with underlying components, and impedance mismatch between power transducers and conditioning circuits.

Impedance matching is complicate for piezoelectric energy harvesting because the source impedance depends on the frequency of the vibrations and the property of the harvester. In order to match the source impedance dynamically, the load needs to change adaptively. DC/DC converters which provide adjustable impedance are therefore proposed for energy harvesting [5][6][7]. In our system, a buck-boost converter running in the discontinuous conduction mode (DCM) directly preceded by a rectifier shown in Figure 5 is used for our system. The DCM buck-boost converter is chosen for the second stage because of its ability to (i) accommodate a wide range of input voltage; and (ii) behave as a lossless resistor to match the source impedance for the maximum power point tracking (MPPT) [8].

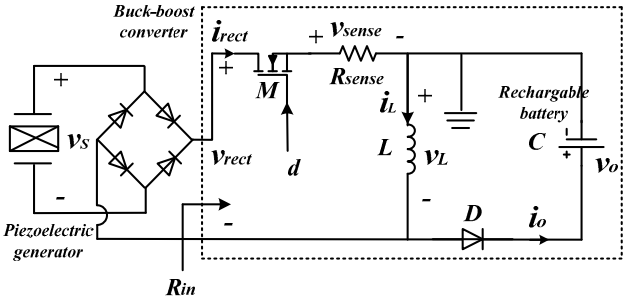

Figure 5. Circuit diagram of the self-powered energy harvesting system

Waveforms for a half cycle of a harmonic base vibration are shown in Figure 6. The effective input resistance of the buck-boost converter is obtained as (3).

$$R_{in} = \frac{v_{rect}}{\frac{1}{T_S}\int_0^{D_1 T_S} i_L dt} = \frac{v_{rect}}{\frac{1}{T_S}\int_0^{D_1 T_S} \frac{v_{rect}}{L} tdt} = \frac{2L}{D_1^2 T_s} \tag{3}$$

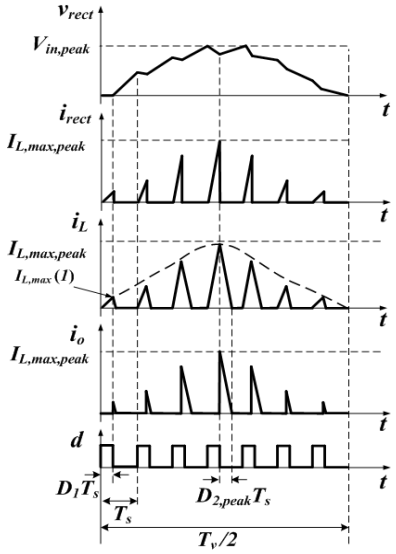

Figure 6. Waveforms during half cycle of a harmonic base vibration

In order to achieve the impedance matching, the effective input resistance R_{in} should be equal to the optimal resistive load $R_{in,opt}$. Hence, the optimal duty cycle can be expressed as

$$D_{1,opt} = \sqrt{\frac{2L}{R_{in,opt} T_s}} \tag{4}$$

For each switching cycle, the input power charges the inductor during switch on-time and releases the inductor energy fully to the load due to the DCM operation. Therefore, the average power delivered to the load for each switching cycle can be expressed as in (5).

$$P_{avg} = \frac{1}{2} L I_{L,\max}^2 F_S \tag{5}$$

To realize the adaptive control of the duty cycle, a microcontroller is configured to sense the input power and adjust the gate control signal of the switch to realize the impedance match. The constant on-time modulation is adopted so that

sensing only the inductor current at the middle point of the switch on-time is sufficient to obtain the average power harvested by the buck-boost converter. The optimal switching frequency for a fixed switch on-time T_{on} can be derived from (4) and is given as

$$F_{S,opt} = \frac{2L}{T_{on}^2 R_{in,opt}} \tag{6}$$

In a practical system, the MPPT algorithm is realized by sensing the current dynamically and modifying the duty cycle adaptively. Figure 7(a) shows the current of the inductor sampled by the current sensing resistor at a constant point of on-time. By comparing the peak values of the current, the controller calculates the average power and decides the tracking direction of the duty cycle. The duty cycle is increased or decreased with a certain fixed increment each time, so that the output power climbs to the maximum point, as shown in Figure 7(b).

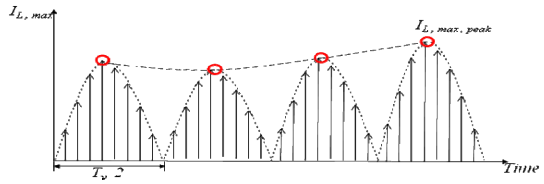

(a)

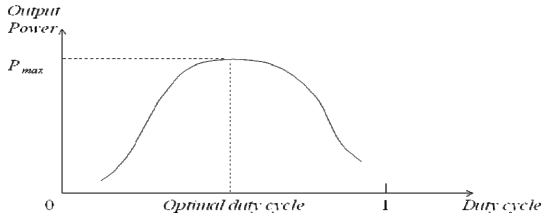

(b)

Figure 7: (a) Sampled inductor current (b) Output power changes with duty cycle

5. SYSTEM INTEGRATION AND IMPLEMENTATION

5.1 System implementation

The self-powered SHM sensor was developed using a TI MSP430 low-power microcontroller from Texas Instruments, which contains an embedded temperature sensor. The maximum clock frequency of MSP430 is 16 MHz. The microcontroller can be programmed to operate in several modes with different levels of power consumption.

The microcontroller evaluation board ez430-RF2500 used for the sensor has a radio called CC2500 operating at 2.4 GHz. The data rate of the radio is programmable and can reach up to 250 kbps, and its coverage is less than 20 meters for an outdoor environment. Also, the radio can be configured to operate in the active mode or sleep mode. It consumes 65 mW during transmission, and as low as 1.2 μW in the sleep mode.

A prototype of the self-powered SHM sensor is shown in Figure 8. It consists of a microcontroller evaluation board, an SHM interface circuit, a power conditioning circuit and a 170 mAh Polymer Li-Ion battery. To save power consumed by analog interface components, a P-channel MOSFET cuts off the power of the interface circuit when it does not perform the SHM operation, i.e., it is in sleep mode. The size of the prototype is 4.5 cm×7 cm× 3 cm. [4]

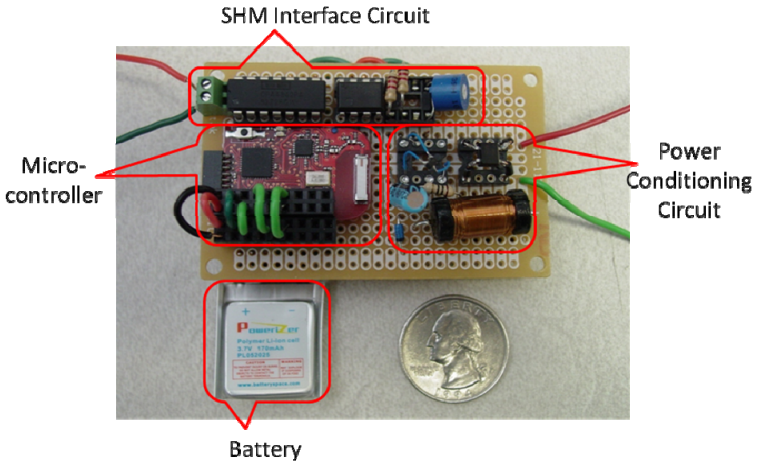

Figure 8: Prototype of a self-powered SHM sensor developed using a TI MSP430 evaluation board

5.2 System operation

Figure 9 shows the system operation of the self-powered SHM sensor. The controller computes the average value of five sampled inductor currents, and increases or decreases the off-time period by 20 µsec at a time based on the average sampled value, while the on-time is fixed to 10 µsec. The direction of the change, increase or decrease of the off-time or the duty cycle, is set to achieve the MPPT. It makes ten such changes before the system goes into the sleep mode, and the MPPT process restarts after 5 seconds.

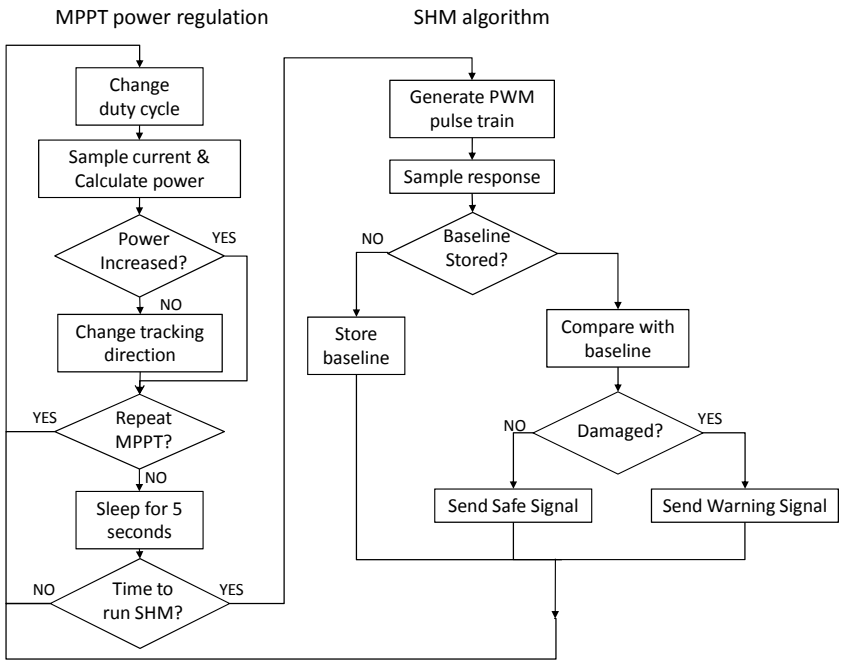

Figure 9: system operation flow of self-powered SHM sensor

SHM operates with a predetermined time period controlled by an internal timer, such as once in several hours or days. The microcontroller sweeps a user specified frequency range and measures the phase profile of a baseline or structure under test (SUT) for the frequency range. It repeats the same operation four times and takes the average value to obtain the phase profile.

The damage metric (DM) for our system is defined as a normalized absolute sum of differences between the phase profiles of the baseline and of the SUT given by

$$\mathrm{DM} = \frac{\sum_{f_i=f_l}^{f_h} \left| \phi_{base}(f_i) - \phi_{SUT}(f_i) \right|}{M(f_l, f_h)} \tag{7}$$

where $M(f_l, f_h)$ is the number of frequency points from the lowest frequency f_l to the highest frequency f_h. The DM of a SUT is compared against a threshold value, whose value may be set based on field experience. If the DM is lower than the threshold value, the SUT is considered healthy. Otherwise, it is damaged. It is important to note that fixed-point calculations without involving multiplications or division are sufficient for Expression (7) provided $M(f_l, f_h)$ is set to power of 2. So, a simple fixed-point processor, rather than a floating-point processor, can be used for our SHM system to save power. Adoption of a more sophisticated DM is possible to improve the SHM performance, but it is not the objective of this design.

6. EXPERIMENTAL RESULTS

6.1 Setup

A. Energy harvesting source

To verify the feasibility of the proposed system, experiments were performed using a cantilevered bimorph generator with a tip mass. The bimorph (manufactured by Piezo Systems, Inc. with model number T226-A4-503X) consists of two oppositely poled PZT-5A piezoelectric elements bracketing a brass substructure layer, and the two piezoelectric elements are connected in series.

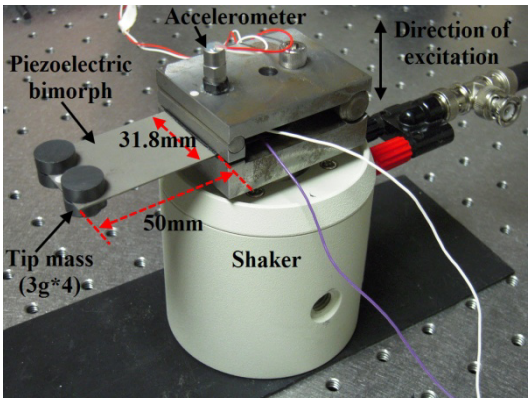

Figure 10. Cantilevered bimorph generator

The optimal resistive load of the piezoelectric cantilever for a given frequency is the one which maximizes the average power output and was identified by tuning the load resistor. The resonant frequency of this setup is about 50 Hz. The optimal resistor varies from 82 to 150 kΩ, while the frequency ranges from 47 to 55 Hz.

B. Test structure

The test structure for our experiments is an aluminum beam with a PZT patch attached at one end. The test structure is hung in free air at the room temperature of around 20° C. A pair of identical magnets are placed on both sides of the beam at a certain position, and the pressure applied to the structure simulates damage. The size of the test beam and four different positions of the two magnets considered for our experiments are shown in Figure 11.

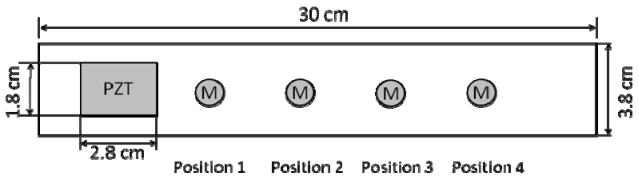

(a) Top view

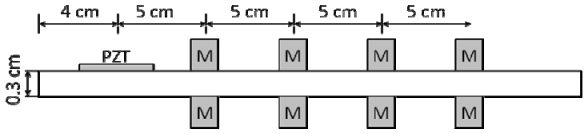

(b) Side view

Figure 11: Test structure and positions of magnets

To identify a sensitive frequency range of the test beam, we measured the impedance of the healthy beam with an impedance analyzer, Agilent 4294A. The impedance profile of the healthy beam is shown in Figure 12. As shown in the figure, the phase of the measured impedance is sensitive in the frequency range from 12 kHz to 35 kHz, and hence the range is set for our experiments.

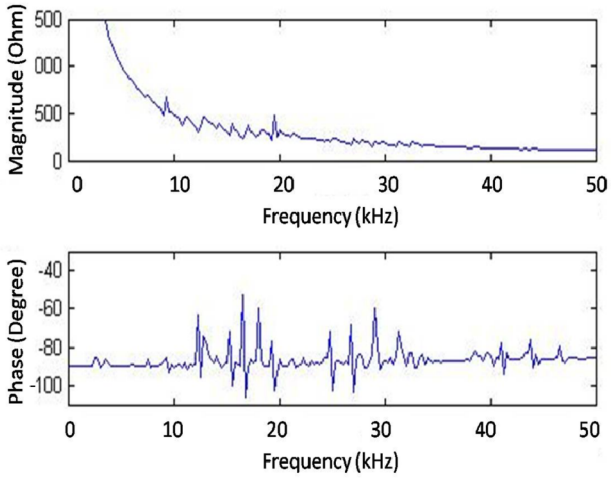

Figure 12: Impedance of the healthy structure

6.2 SHM performance

We performed SHM operations with the SHM sensor, in which the excitation pulse train sweeps from 12 KHz to 35 KHz. Since the phase profile of a SUT changes from one measurement to the next due to noise or other environment changes, we conducted 20 experiments for the baseline and for each damage, i.e., each position of the magnets, and computed the DM values using expression (4). Statistical data for the DM values are tabulated in Table I and presented in Figure 13.

Table I: DM values for 20 experiments

	Baseline	Position 1	Position 2	Position 3	Position 4
Average	3.4	19.2	16.9	15.6	24.2
Maximum	6.7	22.6	17.6	15.9	25.5
Minimum	0.3	18.1	16.3	15.2	23.1
Standard Deviation	1.72	1.29	0.41	0.23	0.79

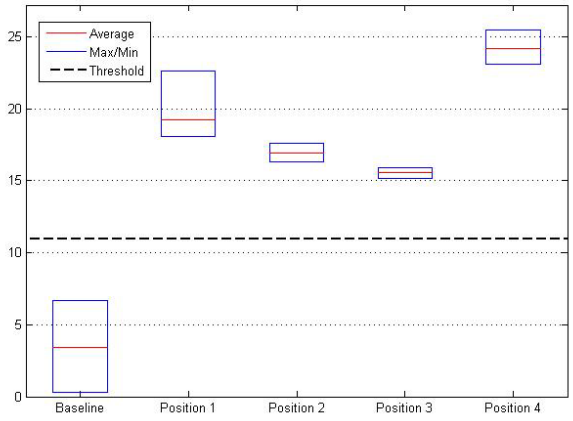

Figure 13: Difference of DM values between the baseline and the four damages

The average DM value of the baseline structure is 3.4, while those for damaged structures range from 15.6 to 24.2. The large difference in the averages values of the baseline and of damaged structures combined with small standard deviations assures detection of damage with high confidence. If the threshold is set between 6.7 and 15.2, the sensor does not incur any false alarm for the particular damages, and the dotted line Figure 11 indicates the optimal DM value (which is the middle point between 6.7 and 15.2). It should be noted that the DM value decreases from Position 1 to Position 3, but increases sharply at Position 4. The result indicates that the proposed damage metric cannot be used to locate damage.

6.3 Power profile

Figure 14 shows the harvested power versus the vibration frequency and the acceleration level of the piezoelectric generator. The harvested power in the figure is computed as (the battery charging power) – (power dissipated by the MCU), in which the power dissipation of the MCU is 0.55 mW. When the harvested power is negative in the figure, the harvested power is insufficient to power up the MCU. The maximum harvested power of 2.9 mW is achieved at the vibration frequency of around 50 Hz under the acceleration of 0.5g (rms).

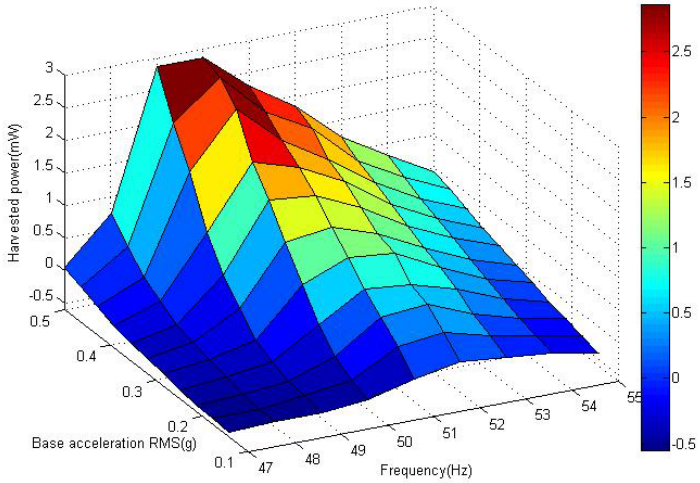

Figure 14. Average power harvested by optimal resistors and the proposed circuit.

The maximum available power is defined as the power delivered to the optimal resistive load connected directly to the piezoelectric generator. The maximum available power under the acceleration of 0.5*g* (rms) is about 4.4 mW for our

system at the resonant frequency of 50 Hz, and the maximum harvested power is 2.9 mW to yield the efficiency of 65%. Some competing circuits report over 60% of efficiency in [7] under the acceleration of 0.5*g* (rms), and below 40% in [6] for the same amount of input power. However, direct comparison of those designs with ours should be judicious due to different environments. For example, [7] does not have a feedback controller, which attributes a substantial power consumption. The circuit in [6] can manage input power as high as 50 mW, which results in a relatively low efficiency for low input power.

Figure 15 shows the outgoing current profile of the battery for our system, while the battery voltage remains constant at 3.52 V during the experiment. Note that the outgoing current from the battery powers up the load including the MCU and the interface circuit, and the energy harvesting circuit except the MCU is powered up by the input power, not the battery. The MCU consumes 385 μW during the sleep mode and 2.2 mW during the execution of the MPPT algorithm. The SHM operation takes 12 seconds, and its average current consumption is 24 mW. The wireless transmission consumes the largest power of 80 mW, but it lasts only 0.03 second. The total energy consumption for one SHM operation is about 0.3 J.

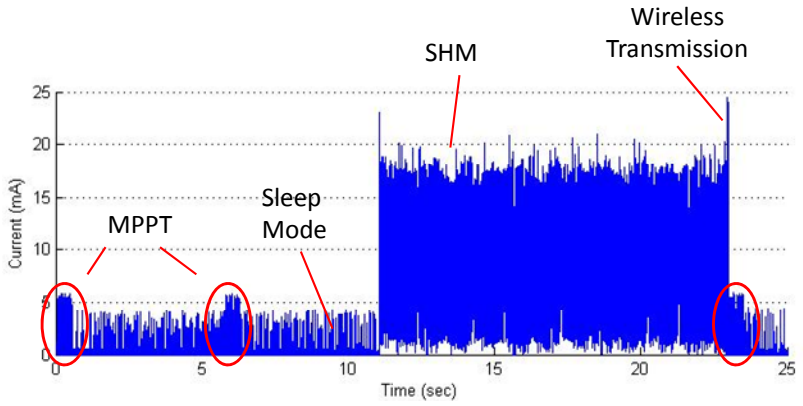

Figure 15: Measured current profile of self-powered sensor

There is a low limit on the interval between two consecutive SHM operations, as the battery should store sufficient energy prior to the next SHM operation. For instance, when the harvested power is 2.9 mW, it takes 105 seconds to store sufficient energy to run the next SHM operation. Thus, the system can run an SHM operation on every 105 seconds. To make our system flexible, the interval between two consecutive SHM operations is programmable.

7. CONCLUSION

In this paper, we presented an impedance-based wireless SHM sensor node integrated with a piezoelectric energy harvester. We reduced power dissipation of our SHM sensor node by adopting on-board processing and eliminating an ADC and the DAC. The piezoelectric cantilever of the system harvests energy from vibrations, and the power conditioning circuit maximizes energy harvesting the an MPPT. Our system was implemented with an TI MSP430 microcontroller evaluation board ez430-RF2500 embedded with CC2500 transceiver. Experimental results show that the SHM sensor node detects local damage efficiently. The system can harvest 2.9 mW under 0.5g (rms) acceleration, which is sufficient to run an SHM operation on every two minutes.

REFERENCES

[1] Kim, J., Grisso, B. L., Ha, D. S., and Inman, D. J., "An All-digital Low-power Structural Health Monitoring System". IEEE Conference on Technologies for Homeland Security, 123-8. (2007).

[2] Kim, J., Grisso, B. L., Ha, D. S., and Inman, D. J., "A System-On-Board approach for Impedance-based Structural Health Monitoring" Proceeding of SPIE, Vol. 6529, 65290O, (2007).

[3] Park, G., Sohn, H., Farrar, C. R., and Inman, D. J., "Overview of piezoelectric impedance-based health monitoring and path forward", The Shock and Vibration Digest, 35, 451-463. (2003).
[4] Zhou, D., Kim, J. K., Bilé, J.-L. K., Shebi, A. B., Ha, D. S. and Inman, D. J., "Ultra Low-Power Autonomous Wireless Structural Health Monitoring Node" Proc. of 7th International Workshop for Structural Health Monitoring, (2009)
[5] G. K. Ottman, H. F. Hofmann, A. C. Bhatt, and G. A. Lesieutre, "Adaptive piezoelectric energy harvesting circuit for wireless remote power supply," IEEE Transactions on Power Electronics, vol. 17, pp. 669-676, (2002)
[6] G. K. Ottman, H. F. Hofmann, and G. A. Lesieutre, "Optimized piezoelectric energy harvesting circuit using step-down converter in discontinuous conduction mode," IEEE Transactions on Power Electronics, vol. 18, pp. 696-703, (2003)
[7] E. Lefeuvre, D. Audigier, C. Richard, and D. Guyomar, "Buck-boost converter for sensorless power optimization of piezoelectric energy harvester," IEEE Transactions on Power Electronics, vol. 22, pp. 2018-25, (2007)
[8] W. Erickson and D. Maksimovic, "Fundamentals of Power Electronics," Norwell, MA: Kluwer, (2001)